THE JOURNAL OF PHYSICAL CHEMISTRY C

Article

pubs.acs.org/JPCC

Understanding the Importance of Carbenium Ions in the Conversion of Biomass-Derived Alcohols with First-Principles Calculations

Pavlo Kostestkyy,[†,#] Jyoti Prakash Maheswari,[†,‡,#] and Giannis Mpourmpakis*[,†]

[†]Department of Chemical Engineering, University of Pittsburgh, Pittsburgh, Pennsylvania 15261, United States

[‡]Department of Chemical Engineering, National Institute of Technology, Warangal 506004, Telangana, India

Supporting Information

ABSTRACT: Dehydration reactions play a key role in the conversion of biomass derivatives to valuable chemicals, such as alcohols to alkenes. Both Lewis and Brønsted acid-catalyzed dehydration reactions of biomass-derived alcohols involve transition states with carbenium ion characteristics. In this work, we employed high-level ab initio theoretical methods to investigate the effect of molecular structure on the physicochemical properties of a set of alcohols that appear to control dehydration chemistry. Specifically, we calculated the carbenium ion stability (CIS, alkene-binding H^+) and proton affinity (PA, alcohol-binding H^+) of various C2−C8 alcohols to show the effect of alcohol size and degree of primary heteroatom substitution on the properties of the reactive species. Our results show a strong linear correlation between CIS and PA, following the substitution order of the reacting alcohols (i.e., primary < secondary < tertiary). Additionally, the calculated binding free energy (BE) of water on the formed carbenium ions was found to be exothermic and to decrease in magnitude with increasing alcohol substitution level. We demonstrate that the CIS and/or the PA are excellent structural descriptors for the alcohols and, most importantly, they can serve as reactivity descriptors to screen a large number of alcohols in the conversion of biomass-based alcohols involving the formation of carbenium ions. We demonstrate this concept in both Lewis and Brønsted acid-catalyzed dehydration reactions.

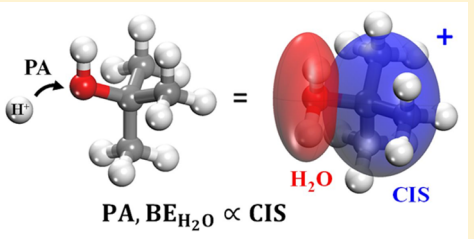

INTRODUCTION

Global primary energy consumption, including commercial renewable energy, increased by 5.6% in 2010, reaching its highest value since 1973. China accounted for 20.3% of the total global energy consumption, followed closely by the United States at 19%.[1] The depleting fossil fuel resources and increasing pollution and global warming concerns require the utilization of alternative and sustainable methods for the production of energy and chemicals.[2] Biomass is an abundant and inexpensive resource with a worldwide production of 560 billion tons of carbon.[3] Biomass-derived energy represents ∼14% of the world's primary energy supply with 25% usage in developed and 75% usage in developing countries. The total sustainable worldwide biomass energy potential is $\sim 2.47 \times 10^{13}$ kJ/m^2, corresponding to a third of the current total global energy consumption.[4] The abundant quantity of biomass and its sustainable nature make it a plausible alternative source of energy and chemicals production (ethanol, lactic acid, acetone, etc.).

Glucose and fructose (major sugars), polyols, and simpler alcohols can be derived from cellulosic biomass processing and further converted into valuable chemicals. For instance, glucose can be reduced to sorbitol, which in turn can be converted to simpler alkanes such as hexane and used as a fuel, through a series of catalyzed dehydration and hydrogenation reactions.[5] Several processes currently exist to convert carbohydrates to liquid fuels. These include (among others) the formation of bio-oils by liquefaction or pyrolysis of biomass,[6] the production of green gasoline, diesel, and other biofuels by applying the Fischer−Torpsch synthesis on biomass-derived syngas (biosyngas),[7] and conversion of sugars and methanol to aromatic hydrocarbons over zeolite catalysts.[8,9] However, the conversion of glucose to ethanol through fermentation remains one of the most widely practiced processes.[10] The utilization of biomass-derived alcohols (e.g., ethanol from biomass fermentation) instead of petroleum-based feedstocks can offset the petroleum load and reduce net CO_2 emissions. Dehydration of alcohols to olefins is an important production route for chemicals, because olefins find a wide range of industrial applications (ethylene, ethylene oxide, etc.).

Solid acid catalysts, such as zeolites, have been used in alcohol dehydration at both laboratory and industrial scales.[11] Dehydration of alcohols via Brønsted acid-catalyzed mechanisms has been extensively studied on solid acids by Gorte et al.[12] The authors proposed a mechanism initiated by alcohol adsorption to form a zeolite-bound oxonium ion, followed by a dehydration step in which water is formed along with a carbenium ion bound to the zeolite surface, which in turn loses a proton to form an olefin (Figure 1a). The transition state for the Brønsted acid-catalyzed dehydration reaction has been postulated to have a partial positive charge, forming a carbenium ion.[12] Additionally, both theory and experiments

Received: May 10, 2015
Revised: June 11, 2015
Published: June 19, 2015

DOI: 10.1021/acs.jpcc.5b04485
J. Phys. Chem. C 2015, 119, 16139−16147

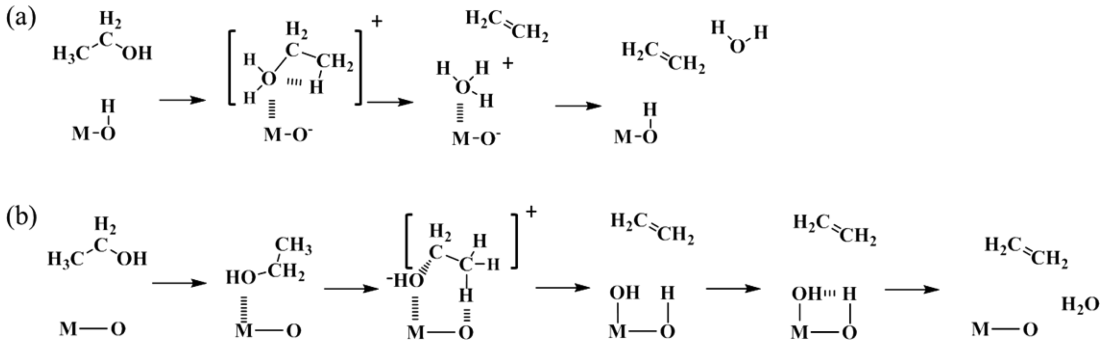

Figure 1. Schematic representations of simplified Brønsted acid-catalyzed alcohol dehydration mechanism on a zeolite active site proposed by Gorte et al.,[12] where M represents the zeolite network (a); concerted E2 elimination mechanism on metal oxides as presented in ref15, where M represents the metal Lewis acid site (b). Relevant transition states with carbenium ion character are highlighted for both mechanisms.

Table 1. Alcohols (C2−C8) Investigated, Including All Isomers of C2−C6 Alcohols and Select C7 and C8 Structures

alcohol no.[a]	alcohol substitution	chain length	name	alcohol no.[a]	alcohol substitution	chain length	name
1	primary	C2	ethanol	22	primary	C6	4-methyl-1-pentanol
2	primary	C3	1-propanol	23	tertiary	C6	2-methyl-2-pentanol
3	secondary	C3	2-propanol	24	secondary	C6	3-methyl-2-pentanol
4	primary	C4	1-butanol	25	secondary	C6	4-methyl-2-pentanol
5*	primary	C4	isobutanol	26	secondary	C6	2-methyl-3-pentanol
6	secondary	C4	2-butanol	27	tertiary	C6	3-methyl-3-pentanol
7	tertiary	C4	*tert*-butanol	28*	primary	C6	2,3-dimethyl-1-butanol
8	primary	C5	1-pentanol	29	primary	C6	3,3-dimethyl-1-butanol
9	primary	C5	3-methyl-1-butanol	30	tertiary	C6	2,3-dimethyl-2-butanol
10*	primary	C5	2-methyl-1-butanol	31*	secondary	C6	3,3-dimethyl-2-butanol
11*	tertiary	C5	2,2-dimethyl-1-propanol	32*	tertiary	C6	2,2-dimethyl-1-butanol
12	secondary	C5	3-pentanol	33*	secondary	C6	cyclohexanol
13	secondary	C5	2-pentanol	34*	primary	C6	2-ethyl-1-butanol
14	secondary	C5	3-methyl-2-butanol	35	primary	C7	1-heptanol
15	secondary	C5	cyclopentanol	36	secondary	C7	2-heptanol
16	tertiary	C5	2-methyl-2-butanol	37	tertiary	C7	2-methylhexan-2-ol
17	primary	C6	1-hexanol	38*	secondary	C7	cycloheptanol
18	secondary	C6	2-hexanol	39	primary	C8	1-octanol
19	secondary	C6	3-hexanol	40	secondary	C8	2-octanol
20*	primary	C6	2-methyl-1-pentanol	41	tertiary	C8	2-methylheptan-2-ol
21	primary	C6	3-methyl-1-pentanol	42*	secondary	C8	cyclooctanol

[a]Asterisk (*) denotes structural rearrangement in the corresponding carbenium ion (vide infra).

suggested that the stability of the formed carbocation in the transition state drives the selectivity in the conversion of polyols as observed by Courtney et al. in the liquid phase dehydration of propylene glycol on Brønsted catalysts (zeolites and Amberlist).[13] Thermodynamically driven pinacol rearrangements of a secondary carbocation in the presence of a catalyst were observed and reported. On the other hand, alcohol dehydration on γ-alumina follows a Lewis acid-catalyzed E2 concerted elimination type of mechanism, as shown by Roy et al.[14] According to this mechanism, a β-hydrogen of the alcohols is transferred to a surface oxygen of the oxide and the C−OH bond of the alcohol is depleted in a concerted reaction step, resulting in alkene formation and water. This mechanism again involves a transition state with carbenium ion characteristics as shown in Figure 1b. The authors concluded that the stability of the carbocation in the transition state plays a significant role in the dehydration of biomass-derived alcohols.

A carbocation is an ion with positive charge on a carbon atom with a vacant p orbital.[16] Carbocations are classified on the basis of the number of valence electrons in the charged carbon atom. For instance, carbocations with three valence electrons are referred to as carbenium ions, whereas structures with five or six valence electrons are classified as carbonium ions.[16,17] Trivalent carbenium ions can be formed by olefin protonation, whereas protonation of saturated alkanes may result in the formation of nonclassical pentacoordinated carbonium ions.[18] For the remainder of this work, the term carbocation is used interchangeably with the term carbenium ion. The carbenium ion structures resemble sp^2 hybridization with a trigonal planar molecular geometry. They exhibit rearrangements,[19] resonance,[20] and hyperconjugation[21] to distribute the positive charge and stabilize the final structure. Carbenium ion stability (CIS) follows a trend of the primary heteroatom substitution: primary < secondary < tertiary. CIS can be quantitatively expressed in terms of the gas phase proton affinity (PA) of the corresponding alkene to form the carbenium ion.[14]

As shown above, carbocations are key intermediates in both Brønsted and Lewis acid-catalyzed alcohol dehydration reactions. The key difference between the two mechanisms is that in the Brønsted, the carbenium ions are stabilized by the

DOI: 10.1021/acs.jpcc.5b04485
J. Phys. Chem. C 2015, 119, 16139−16147

presence of water (protonation of OH-group of the alcohol; see Figure 1a), whereas, in the Lewis, the carbenium ions are formed as part of the C−OH bond elongation (carbenium ion stabilized by OH group; see Figure 1b). Dehydration of alcohols on γ-alumina, catalyzed by Lewis acid sites as suggested by Roy et al.,[14] shows a linear correlation between the dehydration activation energy and the CIS (PA of corresponding alkene). Similarly, work of Gorte et al.[12] on Brønsted acid catalysts shows a linear trend in the heat of formation of the adsorption complex on the catalyst surface and the PA of adsorbates such as alcohols, pyridines, amines, and nitriles. In addition, Janik et al. studied the alcohol dehydration on polyoxometalates and showed that the reaction barriers are linearly related with the deprotonation energy (measure of acid strength) and inversely related with the alcohol PA (base strength).[22] As a result, the dehydration of alcohols involves transition states with carbenium ion characteristics, highlighting the importance of CIS as a quantitative descriptor that determines both the activity and selectivity in the dehydration of alcohols.[12,14,15,23]

In this work, we use highly accurate quantum mechanical methods to calculate (i) the PA of a series of alcohols ranging from C2 to C8 species (H^+ binding on the OH-group) and (ii) their corresponding CIS (H^+ binding on the corresponding olefins). Our results reveal a strong linear correlation between the two properties and a linear correlation between these properties and the calculated dehydration barriers of both Brønsted and Lewis acid-catalyzed mechanisms. Most importantly, this work unravels a way to connect Brønsted and Lewis acid-catalyzed dehydration chemistries and identifies relationships that help us understand activity and selectivity trends in biomass dehydration.

COMPUTATIONAL METHODS

Electronic structure calculations were employed at various levels of theory, namely, B3LYP combined with the 6-311G* basis set,[24] CBS-QB3,[25] and G4[26] as implemented in the Gaussian 09[27] computational package. Structures of C2−C8 species, including alcohols, protonated alcohols, carbenium ions (protonated alkenes), and alkenes, were fully optimized, and the ground states were verified by the absence of any imaginary frequencies. The total (gas phase) Gibbs free energies and enthalpies were calculated at the standard state of T = 298.15 K and P = 1 atm.

We have accounted for all alcohol isomer structures in the C2−C6 size range and representative alcohols (primary, secondary, tertiary, including cyclic) from C7 and C8 alcohols (total of 42 alcohols; see Table 1).

The CIS is calculated in terms of PA of the alkene as

$$\mathrm{CIS} = \mathrm{PA}_{\mathrm{alkene}} = |H_{\mathrm{carbenium\ ion}} - H_{\mathrm{alkene}}| \quad (1)$$

where $H_{\mathrm{carbenium\ ion}}$ and H_{alkene} are the total enthalpies of the carbenium ion and the alkene, respectively.[14] Similarly, we can calculate the free energy change in the CIS as (CIS = $G_{\mathrm{carbenium\ ion}} - G_{\mathrm{alkene}}$). In both cases it has been assumed that the free energy and enthalpy of the proton is zero.

The PA of the alcohol can be defined as the enthalpy (or free energy) change between the protonated and nonprotonated alcohol states.

$$\mathrm{PA}_{\mathrm{alcohol}} = |H_{\mathrm{protonated\ alcohol}} - H_{\mathrm{alcohol}}| \quad (2)$$

The Gibbs free energy (and enthalpy) of the dehydration reaction (eq 3) for the various alcohols was calculated using eq 4.

$$\mathrm{C}_n\mathrm{H}_{2n+1}\mathrm{OH} \rightarrow \mathrm{C}_n\mathrm{H}_{2n} + \mathrm{H}_2\mathrm{O} \quad (3)$$

$$\Delta G_{\mathrm{rxn}} = G_{\mathrm{alkene}} + G_{\mathrm{water}} - G_{\mathrm{alcohol}} \quad (4)$$

The protonated alcohol can be considered as a carbenium ion (CI) stabilized by a water molecule. The binding free energy (BE) of water on the adjacent CI for the protonated alcohols was calculated according to eq 5.

$$\mathrm{BE}_{\mathrm{H_2O}} = G_{\mathrm{protonated\ alcohol}} - G_{\mathrm{carbenium\ ion}} - G_{\mathrm{water}} \quad (5)$$

We can further analyze this relationship by describing the BE as a function of the CIS (calculated in terms of free energy differences) by using eqs 1 and 2 as follows:

$$G_{\mathrm{protonated\ alcohol}} = \mathrm{PA}_{\mathrm{alcohol}} + G_{\mathrm{alcohol}} \quad (6)$$

$$G_{\mathrm{carbenium\ ion}} = \mathrm{CIS} + G_{\mathrm{alkene}} \quad (7)$$

Substituting eqs 6 and 7 into eq 5, we obtain

$$\mathrm{BE}_{\mathrm{H_2O}} = \mathrm{PA}_{\mathrm{alcohol}} + G_{\mathrm{alcohol}} - \mathrm{CIS} - G_{\mathrm{alkene}} - G_{\mathrm{water}}$$

$$\mathrm{BE}_{\mathrm{H_2O}} = \mathrm{PA}_{\mathrm{alcohol}} - \mathrm{CIS} - \Delta G_{\mathrm{dehydration}} \quad (8)$$

As shown in eq 8, $\mathrm{BE}_{\mathrm{H_2O}}$ can be expressed in terms of alcohol CIS, PA, and the net free energy change of the dehydration reaction. This is particularly interesting as it combines multiple key properties of the species involved in alcohol dehydration into a simple algebraic expression. Please note that CIS and the PA values were highly exothermic, but for ease of analysis, absolute values of both CIS and PA were reported.

For all geometry optimizations, the standard convergence criteria of Gaussian were used (max force = 0.00045 au, RMS force = 0.0003 au, max displacement = 0.0018 au, and RMS displacement = 0.0012 au). All transition states in reaction pathways were located by scanning the potential energy surface along the reaction coordinate. The energy maximum that was found along the reaction coordinate was fully relaxed to a saddle point to locate the actual transition state. Transition states (TS) were verified both by the presence of a single imaginary frequency and by intrinsic reaction coordinate (IRC) calculations[28] at the B3LYP/6-311G* level of theory.[24,25]

RESULTS AND DISCUSSION

A number of publications have investigated the proton affinities of alcohols (PA) and alkenes (CIS) using experimental and computational methods.[29−34] Specifically, Hunter et al.[31] have compiled an extensive library of acidity/basicity values for a range of molecules, including alcohols and alkenes. The authors showed composite computational methods such as G2 to consistently predict PA values within ∼10 kJ/mol of experimental values. A comparison of NIST-reported[35] PA values and those calculated in this work, for select primary, secondary, and tertiary alcohols, is shown in Figure 2. Our calculated results agreed with the NIST-reported PA data within 3.4 kJ/mol on average.

CIS and PA values for all of the alcohols summarized in Table 1 were calculated using the three ab initio theoretical methods. Two different values of CIS were found for a number of species, based on the relative stabilities of the deprotonated alkenes, as shown below:

DOI: 10.1021/acs.jpcc.5b04485
J. Phys. Chem. C 2015, 119, 16139−16147

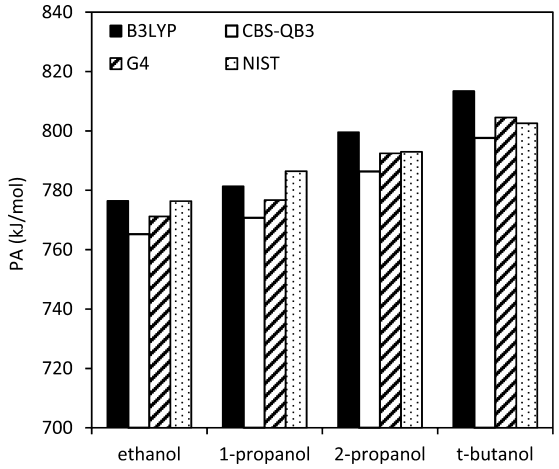

Figure 2. Comparison of calculated (B3LYP, CBS-QB3, and G4) and NIST-reported PA values for ethanol, 1- and 2-propanol, and *tert*-butanol.

$$R{-}CH_2{-}CH{=}CH_2 + H^+ \rightleftharpoons R{-}CH_2{-}C^+H{-}CH_3 \quad (9a)$$

$$R{-}CH{=}CH{-}CH_3 + H^+ \rightleftharpoons R{-}CH_2{-}C^+H{-}CH_3 \quad (9b)$$

Equations 9a and 9b show that the same carbenium ion can be formed by protonation of two different alkenes. For example, Brønsted acid-catalyzed dehydration of 2-butanol proceeds via formation of a protonated alcohol (or water-stabilized carbocation) and formation of two alkene products, (a) 1-butene and (b) 2-butene, along with water. Alkene b exists at a lower total potential energy state than alkene a; as a result, formation of aleken b is more favorable than the formation of alkene a). Generally, more substituted alkenes are favored over less substituted alkenes, and *trans*-alkenes are preferred over *cis*-isomers.[21,36] As the C=C bond is not free to rotate, *cis*-alkenes experience steric hindrance and, hence, are less stable. Also, in more substituted alkenes, the p orbitals of the π-bond are stabilized by the neighboring alkyl substituents. In calculating the stability of such protonated alkenes (carbenium ions), two alkene isomers were possible, resulting in two calculated CIS values. The lower CIS value (reported hereafter) results when accounting for the most stable alkene (isomer) structures, whereas higher CIS account for less stable alkenes.

Figure 3 shows the CIS versus PA values for all alcohols calculated at the B3LYP/6-311G* level of theory, considering the most stable alkene isomers. A linear correlation between CIS and PA was observed at all levels of theory. The values of CIS and PA calculated at the B3LYP level were generally higher (~25 kJ) than in the case of CBS-QB3 and G4. This is consistent with the computational cost and projected accuracy of these methods; that is, CBS-QB3 and G4 provide more accurate thermochemistry results than B3LYP. The results obtained using the CBS-QB3 methodology compared favorably with those at the G4 level, although they were obtained at a slightly reduced computational cost. The full data set for all alcohols at all levels of theory can be found plotted in Figure S01 and tabulated in Tables S07–S09 in the accompanying Supporting Information.

Upon detailed examination of the trends shown in Figure 3a, structural rearrangements were observed for several carbenium ions resulting in deviations from the linear trend (point scatter). The driving force for the rearrangements was the increased stability (lower energy state) in the formation of the carbenium ion that correlates with the degree of substitution of the carbenium ion (i.e., tertiary > secondary > primary). The rearrangements occurred via hydride or methyl shifts, during geometry optimizations of the initially protonated alkene structures, to attain a lower energy isomer. A similar type of carbocation rearrangement is the pinacol rearrangement, as observed in the liquid phase dehydration of propylene glycol on

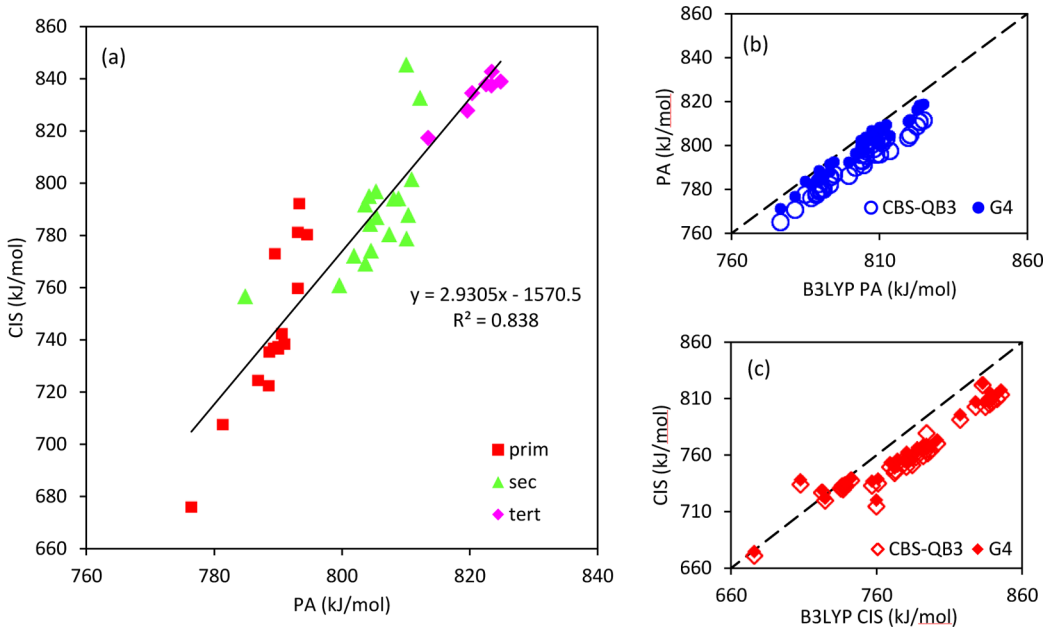

Figure 3. (a) CIS versus PA for all alcohols calculated at the B3LYP/6-311G* level of theory. Parity plots showing the calculated (b) PA and (c) CIS values, with the CBS-QB3 (hollow symbols) and G4 (filled symbols) methods, compared to those calculated at the B3LYP/6-311G* level ($y = x$ line). Red diamonds and blue circles correspond to CIS and PA values, respectively.

DOI: 10.1021/acs.jpcc.5b04485
J. Phys. Chem. C 2015, 119, 16139–16147

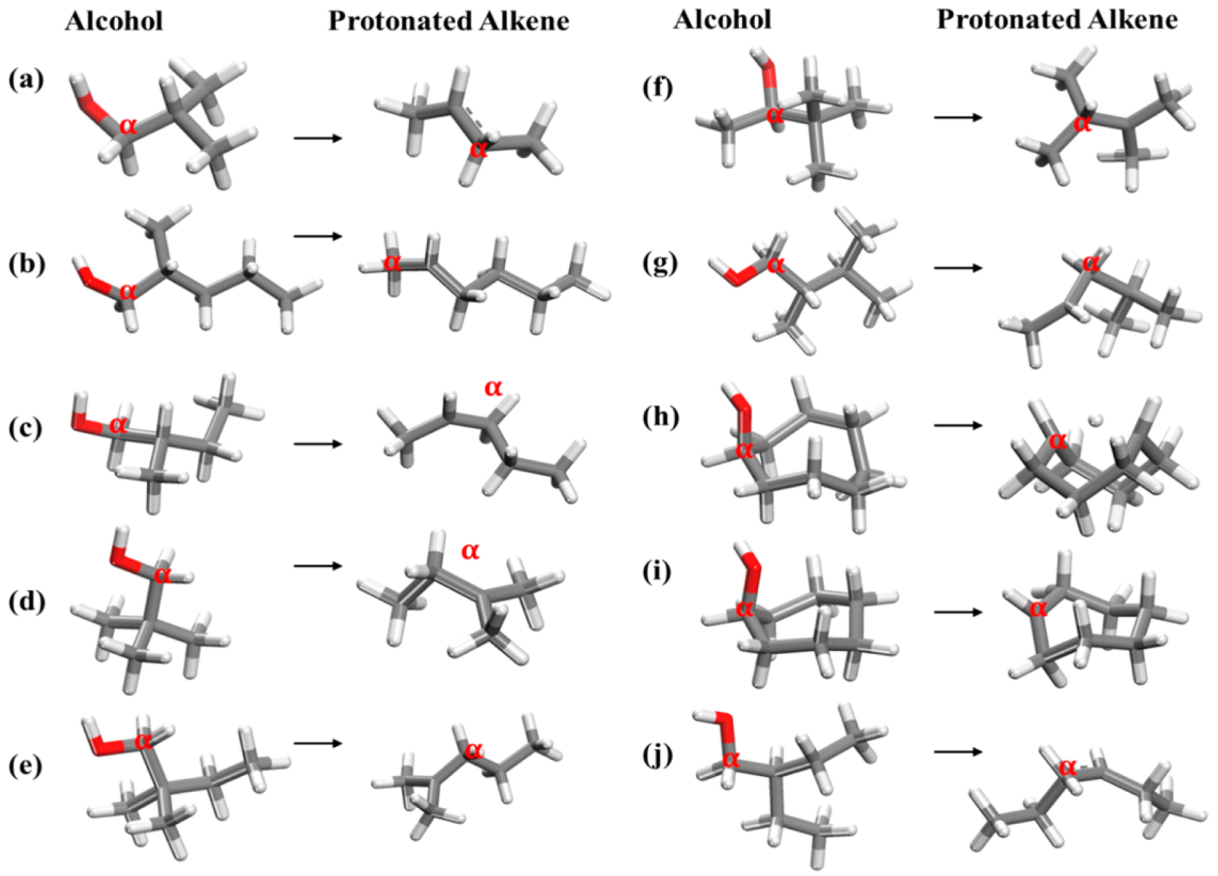

Figure 4. Alcohols and the corresponding carbocation structure after restructuring: (a) isobutanol; (b) 2-methyl-1-pentanol; (c) 2-methyl-1-butanol; (d) 2,2-dimethyl-1-propanol; (e) 2,2-dimethyl-1-butanol; (f) 3,3-dimethyl-2-butanol; (g) 2,3-dimethyl-1-butanol; (h) cyclooctanol; (i) cycloheptanol; (j) 2-ethyl-1-butanol.

solid catalyst.[13] In addition, several protonated cyclic species (cyclohexane, cycloheptane, and cyclooctane) underwent opening of the ring, for the same reasons. Similar ring-opening processes were observed by Feng et al.[23] and Wlodarczyk et al.[37]

The carbocations that underwent structural rearrangements derived from the corresponding alcohols are shown in Figure 4 (the corresponding alcohols are highlighted with asterisks in Table 1). For example, in the case of isobutanol (Figure 4a), we expect a primary carbocation with positive charge localized on C1, but a methyl shift from C2 to C1 resulted in a secondary carbocation with positive charge localized on C2, which is more stable for the reasons stated previously.

Overall, the observed methyl or hydride shifts resulted in higher final complex stability. For example, panels b, c, g, and j of Figure 4 show a methyl shift resulting in a change of a primary carbocation to secondary. In the case of 2,2-dimethylpropanol (Figure 4d) no adjacent H atom existed next to C1 (α-C atom), resulting in a methyl shift from C2 to C1 to form a tertiary CI structure. Similarly, we observed a methyl shift resulting in the transformation of a secondary to tertiary CI for 3,3-dimethyl-2-butanol (Figure 4f). A primary to tertiary CI transformation of 2,2-dimethyl-1-butanol (Figure 4e) was observed. Interestingly, cyclooctanol and cycloheptanol (Figure 4h,i) showed that the cyclic compounds underwent ring opening. The cause of this transformation may be the high angular strain and electronic repulsion required in the attempt to keep ring carbon atoms on a single plane with a positive charge. In the case of cyclooctanol (Figure 4h), the proton is stabilized in the ring center. This results in a higher CIS observed in cyclooctanol, which is of the order of tertiary carbocations. Finally, in the case of ethylene, we observe a proton stabilized between two C atoms, which results in a higher stability of the protonated structure. All of the molecular transformations summarized in Figure 4 result in enhanced CIS values and contribute to the scatter observed in Figure 3a.

When examining the stability of the protonated alkenes (CIS), we observed a higher number of hyperconjugative structures for more substituted alcohols (i.e., tertiary > secondary > primary). In addition, a high inductive effect (+I) from alkyl groups adjacent to the primary carbon atom was observed in the same order, resulting in delocalization and stabilization of the positive charge, making the protonated alkene more stable.

We demonstrate the results of CIS versus PA as presented in Figure 3, at the G4 level of theory, in Figure 5, omitting the cases that resulted in molecular restructuring. In this plot we have highlighted the alcohols as a function of degree of alcohol substitution (primary, secondary, tertiary). It should be noted that the range of the CIS change is approximately 140 kJ/mol, which is larger than that of PA by approximately 40 kJ/mol, as we go from primary to tertiary structures (and increase the chain length). Recall that the PA and CIS values are both exothermic and that their difference decreases as a function of degree of substitution (Figure 5). The most interesting feature of Figure 5 is that the protonation of a hydroxyl group of an alcohol (to form a water-stabilized carbenium ion) is preferred (more exothermic) to the protonation of the olefin to form the

DOI: 10.1021/acs.jpcc.5b04485
J. Phys. Chem. C 2015, 119, 16139−16147

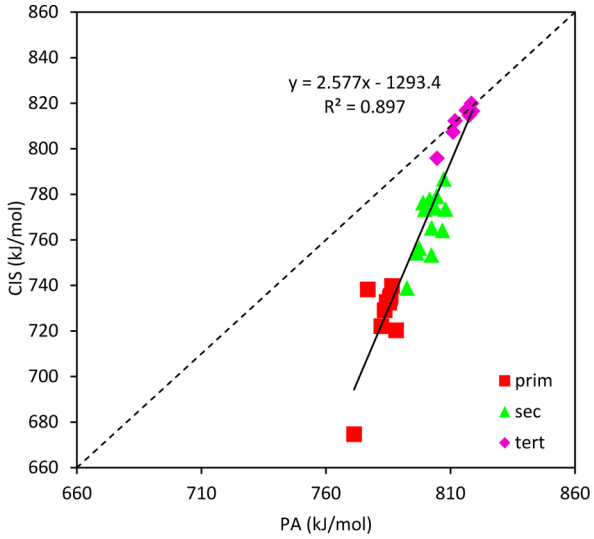

Figure 5. CIS versus PA for primary (red squares), secondary (green triangles), and tertiary (purple rhombs) alcohols, calculated using the G4 method (the dotted line shows $y = x$).

corresponding carbenium ion. This is the case in the formation of primary and secondary carbenium ions, whereas it becomes indifferent (PA = CIS) for the formation of tertiary carbenium ions (purple points fall on the axis $x = y$ in Figure 5). Identical trends were observed for B3LYP and CBS-QB3 computational methods, with detailed results presented in the Supporting Information (Figures S02 and S03).

Alcohol dehydration reaction Gibbs free energies (ΔG_{rxn}) were calculated in the gas phase using eq 4 and plotted as a function of CIS in Figure 6b. A linear-like dependence was observed, however, with significant scatter in the data points. The calculated ΔG_{rxn} values were found to increase (become less favorable) with the degree of alcohol substitution. The dehydration reactions were shown to be exothermic in terms of Gibbs free energies for all primary alcohols and some secondary alcohols at standard conditions. Analysis of reaction enthalpies (ΔH_{rxn}) shown in Figure 6a revealed that all reactions are endothermic with reaction enthalpies ranging from 30 to 80 kJ/mol. The entropic contributions in alcohol dehydration are such that the ΔG_{rxn} values become exothermic for almost all primary alcohols and some of the secondary and remain endothermic for the tertiary alcohols as presented in Figure 6. However, given the relatively low exothermicity/endothermicity in the free energy values of Figure 6b, we can say that overall the reaction appears to be thermoneutral. Detailed computational results for gas-phase alcohol dehydration reaction free energies and enthalpies can be found in Figures S04 and S05, respectively, of the Supporting Information.

Calculated reaction enthalpies and free energies at 298 K for select species (ethanol, 1- and 2-propanol. and *tert*-butanol) were compared to experimental data as shown in Figure 7. We observe good agreement between the computed reaction energies and the ones derived using the NIST database, with an average deviation of 4.3 kJ/mol (Figure 7).

As stated before, the first step in the Brønsted acid-catalyzed alcohol dehydration reaction is the interaction of the alcohol with the acid sites of the catalyst, causing proton transfer and forming a protonated alcohol. A protonated alcohol can be considered as a carbocation stabilized by the presence of a bound water molecule. In dehydration, the water molecule is removed, along with a proton, resulting in the formation of an alkene and water as products (and regenerates the Brønsted acid $- H^+$). According to the results presented in Figure 8, a linear correlation between the BE_{H_2O} and the CIS was observed in the order primary > secondary > tertiary alcohol (the BE_{H_2O} is exothermic, and we show the absolute values). This is not surprising because, as we showed in eq 8, we can describe the BE_{H_2O} as a function of the PA, CIS, and dehydration reaction energy. The latter is very small compared to the PA and CIS values, and because PA is a function of the CIS, the relationship in eq 8 would be a function of a single descriptor, that of the CIS as we show in Figure 8. The observed trends in Figure 8 can be attributed to the stability of the carbenium ion and positive charge localization. For example, in the case of a primary carbenium ion, low carbenium ion stability and localization of positive charge cause the structure to bind water strongly. Charge dispersion and increased carbenium ion stability in the case of secondary and tertiary carbenium ions result in weaker binding of water, as is shown in Figure 8. In the case of tertiary species, very weak interactions with water were

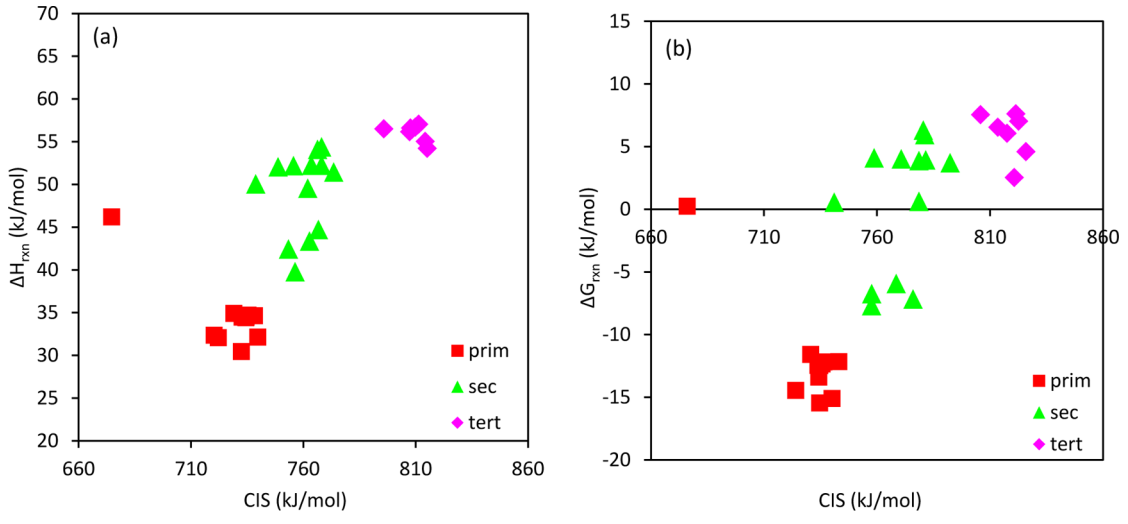

Figure 6. G4 calculated alcohol dehydration reaction enthalpies (a) and free energies (b) versus alcohol CIS.

DOI: 10.1021/acs.jpcc.5b04485
J. Phys. Chem. C 2015, 119, 16139−16147

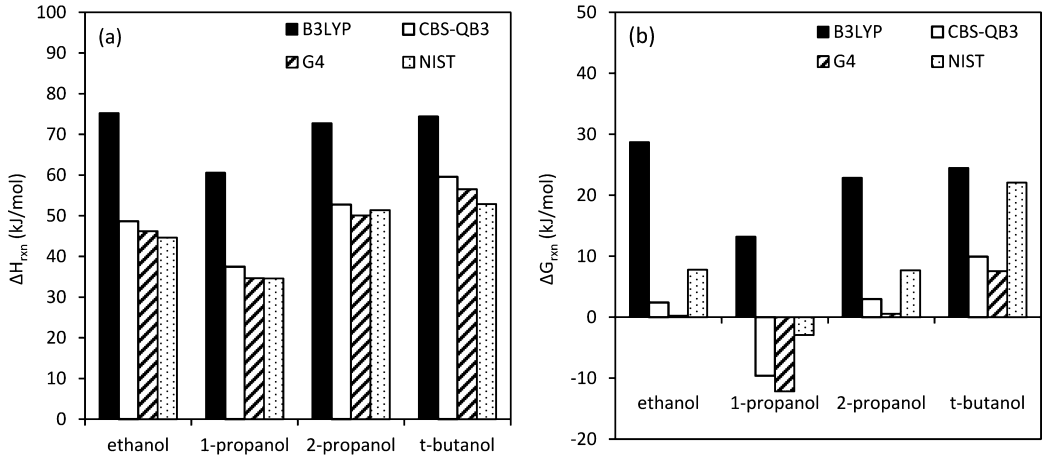

Figure 7. Comparison of calculated enthalpies (a) and Gibbs free energies (b) of reaction with experimental[35] (NIST) values.

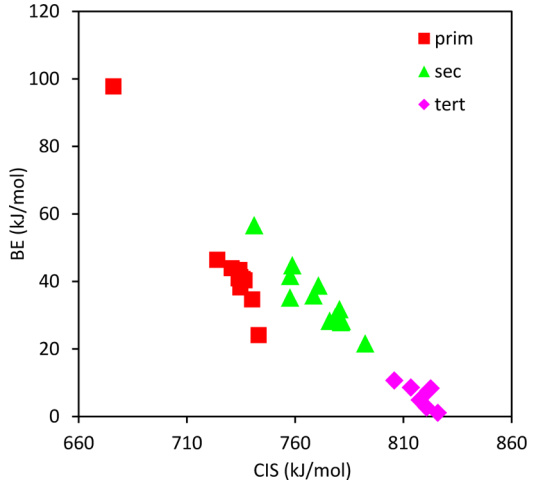

Figure 8. G4 calculated values of BE_{H_2O} versus CIS, with the binding free energies of water (BE_{H_2O}) calculated according to eq 8.

observed, as a result of the increased stability of the tertiary carbenium ion in the gas phase. This is an important observation suggesting that the water removal from the protonated alcohols (presence of Brønsted acids) is thermodynamically difficult for primary alcohols, less so for secondary alcohols, and becomes relatively easy for tertiary alcohols. Identical trends were observed with B3LYP and CBS-QB3 methods as shown in the Supporting Information (Figure S06).

All of the relationships demonstrated so far have been derived on the basis of thermodynamic calculations. We now demonstrate that the stability of the formed carbenium ions plays a key role in the kinetics of the dehydration reactions, and we show that the CIS and the PA of the alcohols can be interchangeably used as descriptors in both Lewis and Brønsted acid-catalyzed dehydration mechanisms. As stated previously, the preferred mechanism in the Lewis acid-catalyzed alcohol dehydration on γ-Al_2O_3 is the concerted E2 mechanism. Additionally, activation energies were shown to decrease with the degree of alcohol substitution, with both computational[15] and experimental means.[14,15,36] We expand this trend to the $Al(OH)_3$, Lewis acid catalyst, and, most importantly, to sulfuric acid, which is a Brønsted acid catalyst.

The dehydration of alcohols in homogeneous acidic media has been shown to evolve via either the E1 or the E2 mechanism.[21] The key difference between the two lies in the nature of the β hydrogen acceptor group, that is, the protonated hydroxyl (OH−H) group or, alternately, the conjugate base, each characterized by their relative basicity. We have investigated both dehydration mechanisms for ethanol, and the detailed reaction pathways are presented in Figure S10 of the Supporting Information. The corresponding transition states in both reaction mechanisms show carbenium ion character. The reaction is initiated by protonation of the weakly basic OH group by the first acidic proton of H_2SO_4. The E2 mechanism involves a concerted step in which the C−O and C−$^{\beta}$H bonds are cleaved simultaneously. Alternatively, the protonated OH−H leaving group separates from the carbon backbone of the alcohol (carbenium ion) and becomes involved in the β-hydrogen transfer step to the newly formed water molecule, according to the E1 mechanism. The E1 mechanism is far more favorable than the E2 in the Brønsted catalyzed mechanism of sulfuric acid. In Figure S11 we present the pathway energetics of the Lewis acid-catalyzed E2 ethanol dehydration mechanism on $Al(OH)_3$. Having identified the energetically preferred pathways for the Lewis and Brønsted acid-catalyzed alcohol dehydration reactions, we relate the calculated dehydration activation energies with the CIS and PA of the different alcohols (Figure 9).

The calculated activation energies correlate linearly both with the CIS and with the PA, clearly capturing the effect of alcohol substitution on the corresponding reaction barriers and are represented by a negative slope of the line. The strong linear correlations are due to the fact that both the E1−Brønsted and the E2−Lewis mechanisms have transition states that exhibit carbenium ion characteristics. Calculated partial charges of the CI in ethanol dehydration were +0.51 and +0.83 |e$^-$| in the Lewis and Brønsted acid-catalyzed transition states, respectively. The reason that these reactivity descriptors (CIS and PA) can be interchangeably used (see Figure 9a,b) is because they are linearly related as we showed in Figure 3. An important observation in Figure 9 is that the Brønsted acid-catalyzed dehydration mechanism shows a higher slope and dependence on the type of the alcohol than the Lewis acid-catalyzed mechanism. Figure 9 denotes that although the Lewis acid-catalyzed dehydration mechanism—at least on these catalysts—is energetically preferred, the Brønsted acid catalyst can achieve higher dehydration selectivities (higher slopes). We are currently investigating if this observation is general and holds on a series of different catalysts.

DOI: 10.1021/acs.jpcc.5b04485
J. Phys. Chem. C 2015, 119, 16139−16147

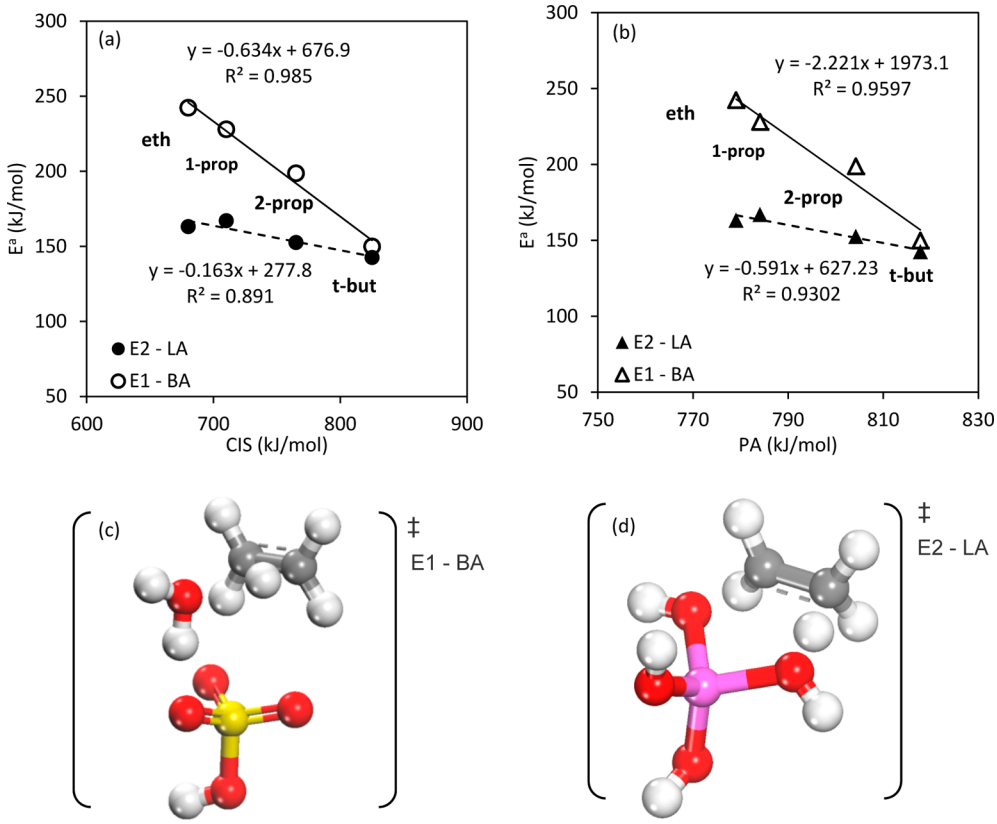

Figure 9. Brønsted acid (BA)- and Lewis acid (LA)-catalyzed activation energies of ethanol, 1-propanol, 2-propanol, and *tert*-butanol, as a function of (a) CIS and (b) PA calculated at the B3LYP/6-311G* level of theory. Linear trends are observed in every case. The corresponding dehydration transition states (shown for ethanol) involving the catalysts H_2SO_4 and $Al(OH)_3$ are demonstrated in panels c and d, respectively.

CONCLUSIONS

First-principles calculations were employed at B3LYP, CBS-QB3, and G4 levels of theory to calculate the gas-phase proton affinities (PA) of C2−C8 biomass-derived alcohols and their carbenium ion stabilities (CIS, proton affinities of corresponding alkenes). The results showed a strong linear correlation between CIS and PA. Both properties (CIS and PA) increase with the degree of alcohol substitution (tertiary > secondary > primary). The specific correlation revealed from this work is important in relating both the Lewis and Brønsted acid-catalyzed dehydration barriers with the PA and CIS properties due to the carbenium ion formation in the transition state of both mechanisms. Overall, the PA > CIS for primary and secondary alcohols and becomes equivalent (PA = CIS) for tertiary alcohols. This shows that protonation of a hydroxyl group is generally more favorable than the protonation of a double bond in hydrocarbons. Hydride and alkyl shifts were observed in some carbocation rearrangements driven by the stabilization of the final carbocation structure.

The change in the Gibbs free energy for the dehydration reactions was calculated to be slightly exothermic for primary and several secondary alcohols, whereas the values were slightly endothermic for some secondary and all tertiary alcohols. The binding energies of water on the formed carbenium ions were calculated. It was shown that primary alcohols bind water the strongest, followed by secondary and tertiary alcohols, suggesting that water removal from the protonated alcohols is thermodynamically most difficult for primary alcohols, followed by the secondary and then by the tertiary alcohols.

Most importantly, the CIS and the PA of the alcohols can be interchangeably used as reactivity descriptors in both Brønsted and Lewis acid-catalyzed dehydration reactions because both properties are linearly related. All of these observations are important in the development of structure−activity relationships in biomass conversion[15] and, specifically, in understanding activity and selectivity in both Lewis and Brønsted-acid catalyzed alcohol dehydration.

ASSOCIATED CONTENT

Supporting Information

CIS, PA, ΔG_{rxn}, ΔH_{rxn}, BE, and E^a values calculated at all levels of theory, including potential energy diagrams of Bronsted and Lewis acid-catalyzed (E1 and E2) dehydration mechanisms. The Supporting Information is available free of charge on the ACS Publications website at DOI: 10.1021/acs.jpcc.5b04485.

AUTHOR INFORMATION

Corresponding Author

*(G.M.) E-mail: gmpourmp@pitt.edu.

Author Contributions

#P.K. and J.P.M. contributed equally to this work.

Notes

The authors declare no competing financial interest.

ACKNOWLEDGMENTS

We acknowledge the Center for Simulation and Modeling (SAM) at the University of Pittsburgh for computational support and start-up funding from the University of Pittsburgh.

DOI: 10.1021/acs.jpcc.5b04485
J. Phys. Chem. C 2015, 119, 16139−16147

J.P.M. acknowledges the National Institute of Technology, Warangal, India, for financial support.

REFERENCES

(1) Izhar, Q.; Fahimuddin, S. Analysis of Global Energy Consumption Patterns. *J. Environ. Res. Dev.* **2013**, *7*, 1761−1773.
(2) Vlachos, D. G.; Caratzoulas, S. The Roles of Catalysis and Reaction Engineering in Overcoming the Energy and the Environment Crisis. *Chem. Eng. Sci.* **2010**, *65*, 18−29.
(3) Groombridge, B.; Jenkins, M. D. *Global Biodiversity: Earth's Living Resources in the 21st Century*; University of California Press: Oakland, CA, USA, 2000; p 11
(4) Parikka, M. Global Biomass Fuel Resources. *Biomass Bioenergy* **2004**, *27*, 613−620.
(5) Huber, G. W.; Dumesic, J. A. An Overview of Aqueous-Phase Catalytic Processes for Production of Hydrogen and Alkanes in a Biorefinery. *Catal. Today* **2006**, *111*, 119−132.
(6) Elliott, D. C.; Beckman, D.; Bridgwater, A. V.; Diebold, J. P.; Gevert, S. B.; Solantausta, Y. Developments in Direct Thermochemical Liquefaction of Biomass: 1983−1990. *Energy Fuels* **1991**, *5*, 399−410.
(7) Hu, J.; Yu, F.; Lu, Y. Application of Fischer−Tropsch Synthesis in Biomass to Liquid Conversion. *Catalysts* **2012**, *2*, 303−326.
(8) Chen, N. Y.; Degnan, T. F.; Koenig, L. R. Liquid Fuel from Carbohydrates. *CHEMTECH* **1986**, *16*, 506−511.
(9) Weisz, P. B.; Haag, W. O.; Rodewald, P. G. Catalytic Production of High-Grade Fuel (Gasoline) from Biomass Compounds by Shape-Selective Catalysis. *Science* **1979**, *206*, 57−58.
(10) Katzen, R.; Tsao, G. T. A View of the History of Biochemical Engineering. *Adv. Biochem. Eng./Biotechnol.* **2000**, *70*, 77−91.
(11) Takahara, I.; Saito, M.; Inaba, M.; Murata, K. Dehydration of Ethanol into Ethylene over Solid Acid Catalysts. *Catal. Lett.* **2005**, *105*, 249−252.
(12) Gorte, R. J. What Do We Know About the Acidity of Solid Acids? *Catal. Lett.* **1999**, *62*, 1−13.
(13) Courtney, T. D.; Nikolakis, V.; Mpourmpakis, G.; Chen, J. G.; Vlachos, D. G. Liquid-Phase Dehydration of Propylene Glycol Using Solid-Acid Catalysts. *Appl. Catal., A* **2012**, *449*, 59−68.
(14) Roy, S.; Mpourmpakis, G.; Hong, D.-Y.; Vlachos, D. G.; Bhan, A.; Gorte, R. J. Mechanistic Study of Alcohol Dehydration on γ-Al_2O_3. *ACS Catal.* **2012**, *2*, 1846−1853.
(15) Kostestkyy, P.; Yu, J.; Gorte, R. J.; Mpourmpakis, G. Structure−Activity Relationships on Metal-Oxides: Alcohol Dehydration. *Catal. Sci. Technol.* **2014**, *4*, 3861−3869.
(16) Gold, V., Loening, K. L., McNaught, A. D., Sehmi, P., Eds. *Compendium of Chemical Terminology Iupac International Union of Pure and Applied Chemistry Recommendations*; Blackwell Scientific: Oxford, UK, 1987.
(17) Boronat, M.; Corma, A. Are Carbenium and Carbonium Ions Reaction Intermediates in Zeolite-Catalyzed Reactions? *Appl. Catal., A* **2008**, *336*, 2−10.
(18) Olah, G. A.; Suryaprakash, G. K.; Sommer, J. Superacids. *Science* **1979**, *206*, 13−20.
(19) March, J.; Smith, M. B. *March's Advanced Organic Chemistry*; Wiley: Hoboken, NJ, USA, 2007; ISBN 0-471-85472-7.
(20) Pauling, L. Citation Classic − the Nature of the Chemical-Bond and the Structure of Molecules and Crystals − an Introduction to Modern Structural Chemistry. *Curr. Contents/Eng. Technol. Appl. Sci.* **1985**, 16−16.
(21) McMurry, J. *Organic Chemistry: A Biological Approach*; Thomson Brooks/Cole: Belmont, CA, USA, 2007.
(22) Janik, M. J.; Macht, J.; Iglesia, E.; Neurock, M. Correlating Acid Properties and Catalytic Function: A First-Principles Analysis of Alcohol Dehydration Pathways on Polyoxometalates. *J. Phys. Chem. C* **2009**, *113*, 1872−1885.
(23) Feng, S.; Bagia, C.; Mpourmpakis, G. Determination of Proton Affinities and Acidity Constants of Sugars. *J. Phys. Chem. A* **2013**, *117*, 5211−5219.
(24) Becke, A. D. Density-Functional Thermochemistry. 3. The Role of Exact Exchange. *J. Chem. Phys.* **1993**, *98*, 5648−5652.
(25) Montgomery, J. A.; Frisch, M. J.; Ochterski, J. W.; Petersson, G.; Alfonso, D. A Complete Basis Set Model Chemistry. VI. Use of Density Functional Geometries and Frequencies. *J. Chem. Phys.* **1999**, *110* (6), 2822−2827.
(26) Curtiss, L. A.; Redfern, P. C.; Raghavachari, K. Gaussian-4 Theory. *J. Chem. Phys.* **2007**, *126*, 12.
(27) Frisch, M. J.; Trucks, G. W.; Schlegel, H. B.; Scuseria, G. E.; Robb, M. A.; Cheeseman, J. R.; Scalmani, G.; Barone, V.; Mennucci, B.; Petersson, G. A., et al. *Gaussian 09*; Gaussian, Inc.: Wallingford, CT, USA, 2009.
(28) Hratchian, H. P.; Schlegel, H. B. Accurate Reaction Paths Using a Hessian Based Predictor-Corrector Integrator. *J. Chem. Phys.* **2004**, *120*, 9918−9924.
(29) Benoit, F. M.; Harrison, A. G. Predictive Value of Proton Affinity − Ionization-Energy Correlations Involving Oxygenated Molecules. *J. Am. Chem. Soc.* **1977**, *99*, 3980−3984.
(30) Holmes, J. L.; Aubry, C.; Mayer, P. M. Proton Affinities of Primary Alkanols: An Appraisal of the Kinetic Method. *J. Phys. Chem. A* **1999**, *103*, 705−709.
(31) Hunter, E. P. L.; Lias, S. G. Evaluated Gas Phase Basicities and Proton Affinities of Molecules: An Update. *J. Phys. Chem. Ref. Data* **1998**, *27*, 413−656.
(32) Nguyen, C. M.; Reyniers, M.-F.; Marin, G. B. Theoretical Study of the Adsorption of the Butanol Isomers in H-Zsm-5. *J. Phys. Chem. C* **2011**, *115*, 8658−8669.
(33) Pau, J. K.; Kim, J. K.; Caserio, M. C. Mechanisms of Ionic Reactions in Gas-Phase - Displacement-Reactions at Carbonyl Carbon. *J. Am. Chem. Soc.* **1978**, *100*, 3831−3837.
(34) Wolf, J. F.; Staley, R. H.; Koppel, I.; Taagepera, M.; McIver, R. T.; Beauchamp, J. L.; Taft, R. W. Gas-Phase Basicities and Relative Proton Affinities of Compounds between Water and Ammonia from Pulsed Ion-Cyclotron Resonance Thermal Equilibria Measurements. *J. Am. Chem. Soc.* **1977**, *99*, 5417−5429.
(35) Linstrom, P. J.; Mallard, W. G. *NIST Chemistry Webbook*; NIST Standard Reference Database [online]; National Institute of Standards and Technology: Gaithersburg, MD, USA, 2011.
(36) Kang, M. J.; DeWilde, J. F.; Bhan, A. Kinetics and Mechanism of Alcohol Dehydration on γ-Al_2O_3: Effects of Carbon Chain Length and Substitution. *ACS Catal.* **2015**, *5*, 602−612.
(37) Wlodarczyk, P.; Paluch, M.; Hawelek, L.; Kaminski, K.; Pionteck, J. Studies on Mechanism of Reaction and Density Behavior During Anhydrous D-Fructose Mutarotation in the Supercooled Liquid State. *J. Chem. Phys.* **2011**, 134.

DOI: 10.1021/acs.jpcc.5b04485
J. Phys. Chem. C 2015, 119, 16139−16147